Design of a Compact Tri-Band PIFA Based on Independent Control of the Resonant Frequencies

Dong-yeon Kim, Jae W. Lee, *Member, IEEE*, Choon Sik Cho, *Member, IEEE*, and Taek K. Lee, *Member, IEEE*

***Abstract*—The application of multiple folded radiator to independent frequency control of a compact tri-band planar inverted-F antenna (PIFA) composed of three resonant frequencies, Global System for Mobile communication (GSM900, 880–960 MHz)/Digital Communication System (DCS1800, 1710–1880 MHz)/Satellite Digital Mobile Broadcasting (Satellite DMB, 2605–2655 MHz) are treated with the optimized parameter values. The proposed antenna has been designed and analyzed by using commercially available softwares, CST MWS based on the finite-difference time-domain algorithm, High Frequency Structure Simulator (HFSS) based on the finite element method algorithm and a simple resonant equation, respectively. It is also seen that good isolation characteristics and independent frequency control can be accomplished by using the separation of folded parts operating at each different frequency. In addition, the return loss has been measured and compared between measured and simulated data under the criterion of VSWR less than 3. The radiation patterns in each service are the same as the omnidirectional characteristics and the maximum gains are 1.19, 2.93, and 1.48 dBi at 0.92, 1.8, and 2.63 GHz, center frequencies of each service, respectively.**

***Index Terms*—Parasitic elements, planar inverted-F antenna (PIFA), tri-band.**

I. Introduction

WITH THE HELP of the rapid development of wireless communication systems and the increasing requirements for portable characteristics of electronic devices, a compact and light-weighted antenna is continuously introduced in many literatures [1]–[10]. Furthermore, in order to satisfy the various demands for wireless services, multiband antenna is a good candidate and planar inverted-F antenna (PIFA) concepts is adopted for antenna design. As a disadvantage of microstrip antenna, it has a narrow bandwidth. In order to overcome the posed problem, PIFA, which is a modification of a vertically installed monopole antenna and has a very high spatial efficiency, has been suggested by inserting shorting strip or shorting pin [1]. However, one of many advantages of PIFA structure is that it can be easily incorporated into the electronic equipments due to the flexible structures and compactness. Thus many researchers have studied the derivation of multiple resonances and low-profile structure by using slit, slot [2]–[4], parasitic elements [5], [6], and the modification of ground pattern [7].

Manuscript received November 21, 2007.

The authors are with the School of Electronics, Telecommunication and, Computer Engineering, Korea Aerospace University, Goyang, Gyeonggi-Do, 412-791, Korea (e-mail: jwlee1@hau.ac.kr).

Color versions of one or more of the figures in this paper are available online at http://ieeexplore.ieee.org.

Digital Object Identifier 10.1109/TAP.2008.922667

Two shorting strips and slits have been introduced to obtain the three resonant frequency bands [2]. Main patch consisting of meander-typed slit occupies the volume of antenna, $40 \times 38 \times 9\,\mathrm{mm}^3$ showing a little larger dimension. On the other hand, it is shown that the lower and upper frequencies of a conventional PIFA can be controlled by using a U-shaped slot on the radiating element [3]. In addition to that, to cover the multiband services, L-shaped patch with two slant slits at the right edge is added [4]. As a different approach to design multiband antenna, parasitic elements instead of slits and slots have been introduced to improve impedance bandwidth. By properly arranging three parasitic elements, which result in three resonant frequencies at each service, respectively, around main patch, multiresonance can be induced and wide impedance bandwidth can be accomplished [5]. As a similar technique, two coplanar parasitic patches are employed to lower the low frequency of the upper frequency band enhancing the impedance bandwidth [6]. In order to investigate the effects of ground plane on the electrical performances of PIFA, a slotted and meandered ground plane has been introduced to achieve the size-reduction of overall antenna volume [7].

From the previous works and literatures related with the design of multiband antenna, it is observed that the main goal is focused on the accomplishment of the easy control of each resonant frequency and the bandwidth of each band. Generally, all of the parameters determining the electrical performances of PIFA have a complex relationship each other, hence it is not easy to control the service bands with multiband characteristics independently. In other words, if a change of certain parameters comprising the radiating structures could have an effect on the other resonant frequencies, the design procedure of the antenna would be very complicated and tedious.

In this paper, two basic meander and folded structures have been applied to accomplish the novel and compact antenna. Folding the meander structure vertically, which occupies $30 \times 16 \times 9\ \mathrm{mm}^3 = 4320\ \mathrm{mm}^3$, leads to a relative volume reduction of 50% by overcoming the problem of low-frequency resonance dependent on the large area of the radiator. This paper deals with the physical insight into the PIFA design covering GSM900 (880–960 MHz), DCS1800 (1710–1880 MHz), and Satellite DMB (2605–2655 MHz). Each radiating part is independently designed and electrically isolated such that the mutual coupling effects can be minimized and the structural independence can be maintained. As an advantage of the proposed antenna, it is very easy to construct this antenna by properly inserting the slits on main radiating patch and introducing folded parts on both side edges.

In Sections II and III, the entire structure of the proposed antenna is described in detail and the simulated results with

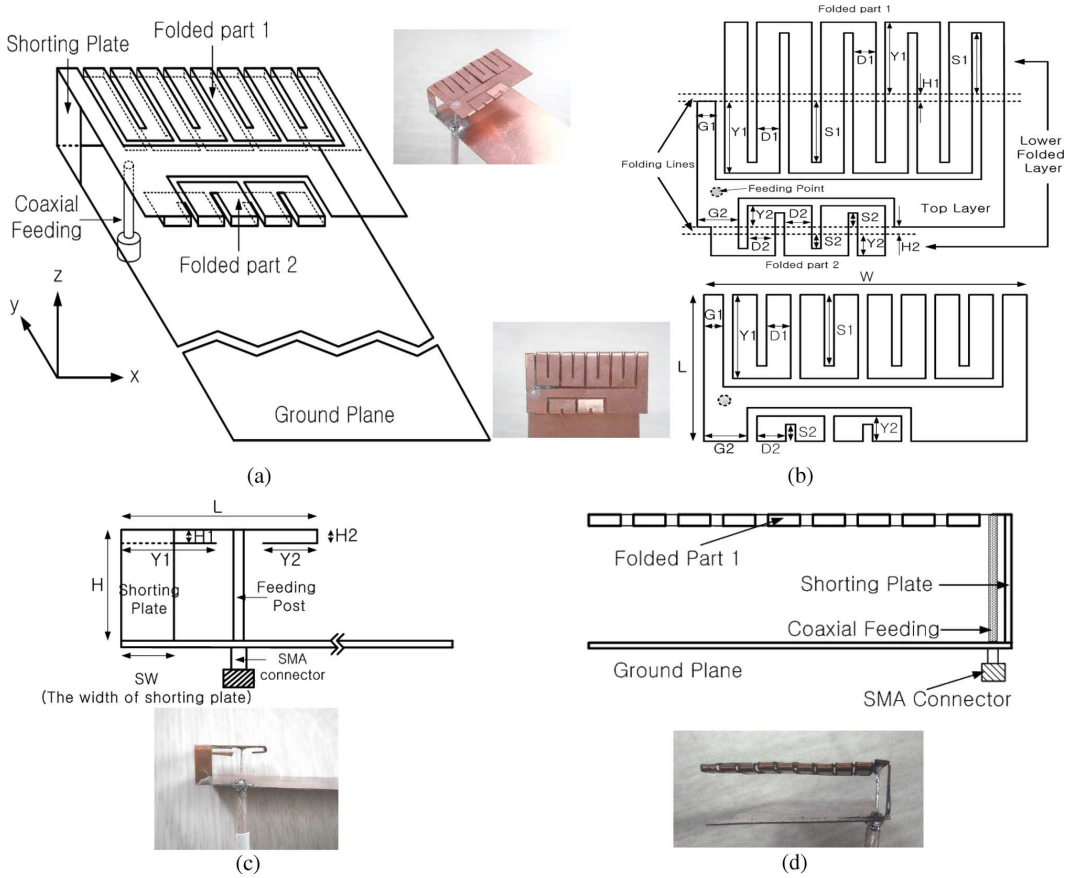

Fig. 1. Antenna geometry and photographs. (a) Perspective view. (b) Top view. (c) Side view. (d) Back view.

the evaluated parameter values are listed using two commercially available softwares with antenna design procedure, respectively. The accuracy of designed parameter values and verification of our design procedure are carried out with measurements in Section IV. Finally, conclusions are briefly shown in Section V.

II. Antenna Configuration

Consider the planar inverted-F antenna having two meander-folded structures installed on the upper and lower edge line separately as shown in Fig. 1. As a description for the given structure, Fig. 1(a) shows the entire structure with a perspective view and Fig. 1(b) depicts the radiating parts (folded parts 1 and 2) governing the resonant frequencies in detail with unfolded layout. Particularly, the unfolded layout helps us understand the connection status between top and lower folded layers. Finally, Fig. 1(c) and (d) show side view and back view of the proposed antenna, respectively. The heights, H1 and H2 of the meandered structure are set to be 1 mm to satisfy the target frequency and wide impedance bandwidth around the resonant frequencies. The 50-Ω cable-feeding structure has been adopted to utilize the limited space effectively and avoid microstrip feed line.

Two meander-folded structures (folded parts 1 and 2) have been employed to induce multiple resonances at different frequencies. The folded part 1 is related with GSM900 band while the folded part 2 can control the Satellite DMB band. The resonant frequency of DCS1800 is dependent on the total area of top plate. The important parameters that determine the resonant frequency of GSM900 are D1, S1, and Y1, which are used in both top and lower folded layers as shown in Fig. 1(b). The optimized parameter values have been obtained from iterative simulation with initial data depending on the relationship between the resonant frequency and the path length of current distribution. In a similar way, the resonant frequency of Satellite DMB can be controlled by finely tuning the parameters, D2, S2, and Y2 with additional parameter G2. At this time, tuning parameters D2, S2, and Y2 are employed to both top and lower folded layers for the better electrical performances. Therefore the total volume through the optimized process amounts to $30 \times 16 \times 9\ \mathrm{mm}^3$.

As controllable parameters related with impedance matching, the position and width of shorting plate play an important role of satisfying the required bandwidth. The designed and optimized parameter values are listed in Table I.

III. Antenna Design Procedure

In this section, the design procedures for the proposed antenna are described. The antenna characteristics are in general affected by the complicated mechanism and the various parameters simultaneously. However it is suggested that the design parameters affecting on each frequency band are located independently and the design process is very easy due to the independent frequency control of resonant target frequencies.

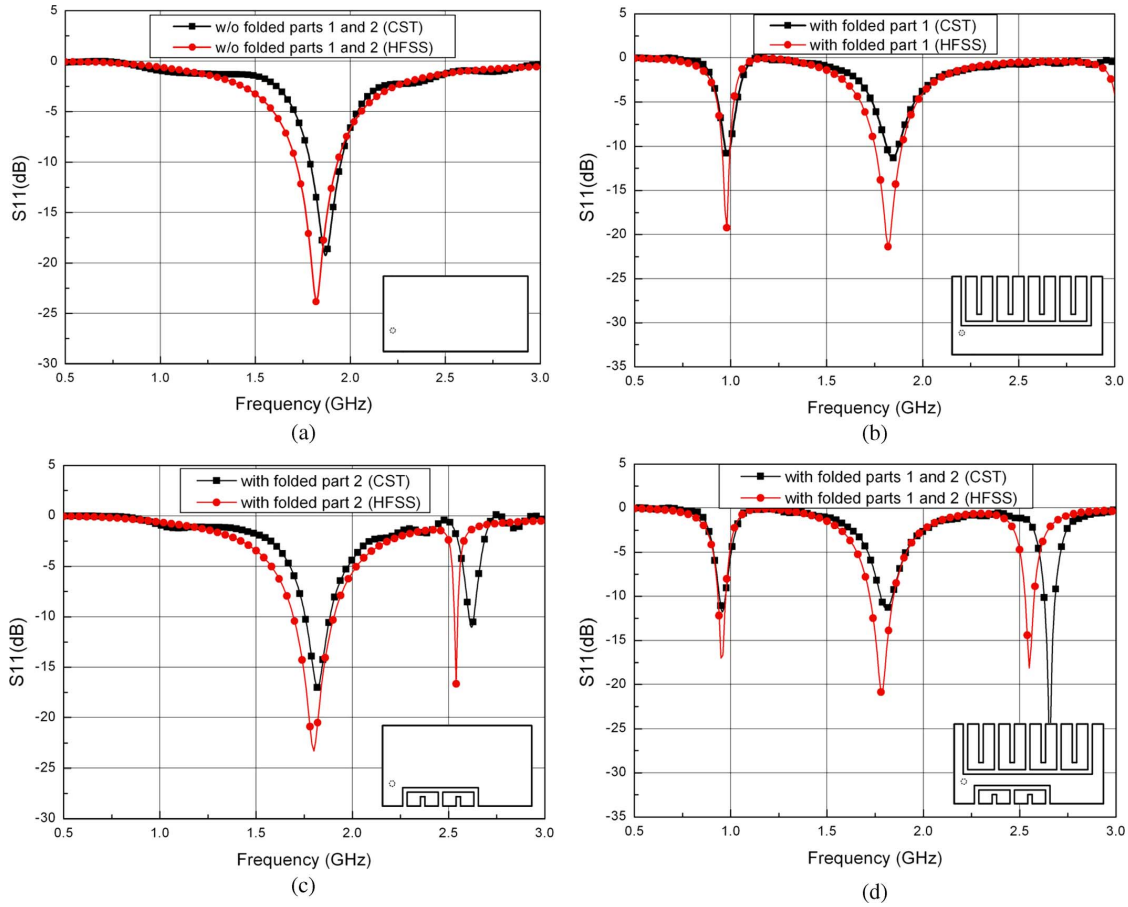

Fig. 2. Return loss as a function of frequency according to the different radiating structures: (a) without the folded parts, (b) with the folded part 1 only, (c) with the folded part 2 only, and (d) with both the folded parts 1 and 2.

TABLE I
DESIGNED PARAMETER VALUES OF THE PROPOSED ANTENNA

Parameter	L	W	G1	G2	H	H1	H2
Value (mm)	16	30	2.1	5	9	1	1
Parameter	D1	D2	S1	S2	SW	Y1	Y2
Value (mm)	2.5	3	7.3	2	5	9	3.8

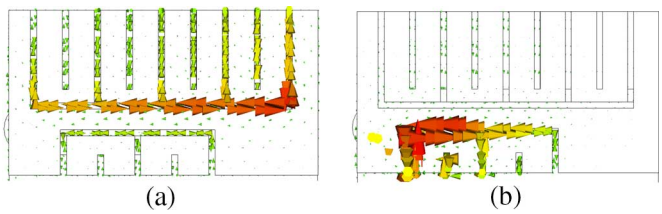

Fig. 3. Current distributions flowing down the structure at GSM900 ($f = 0.92$ GHz) and Satellite DMB ($f = 2.63$ GHz): (a) on the folded part 1 and (b) on the folded part 2.

By applying the basic resonant structure (only top plate) and the structures involving folded parts 1 and 2 to the PIFA successively, the independent and optimized parameters have been obtained for satisfying the requirement of return loss.

A. The Effects of Main Top Patch

PIFA consists of a ground plane, a top plate, a feeding connected between ground plane and top plate, and a shorting wire or plate also connected between ground plane and top plate. However, since the shorting plate is better than the shorting wire to accomplish wide impedance bandwidth, shorting plate with 5 mm plate width through iterative simulation process has been employed in this paper [8]. As a first step to design tri-band antenna, this section describes that the resonant fundamental mode can be designed by using formula relating the resonant frequency with the total area of top plate [10]. In addition, the fine tuning of the length, width, and the location of feeding and shorting plate results in the final targeted frequencies, DCS1800 frequency band with top plate size, $30 \times 16 \times 9$ mm^3.

As a response according to the geometrical structures, Fig. 2(a) shows that the total size of only top plate generates single resonant frequency around 1800 MHz with a good agreement between two simulation results.

B. The Effects of the Folded Part 1 Only

This section describes the design procedure to induce the resonant frequency of the lowest frequency band, GSM900 (880–960 MHz) among three target frequencies. Adopting the meander structure and additional folded part on the upper side edge of the top plate leads the resonant frequency at GSM900 and increases the spatial efficiency. From the previous studies

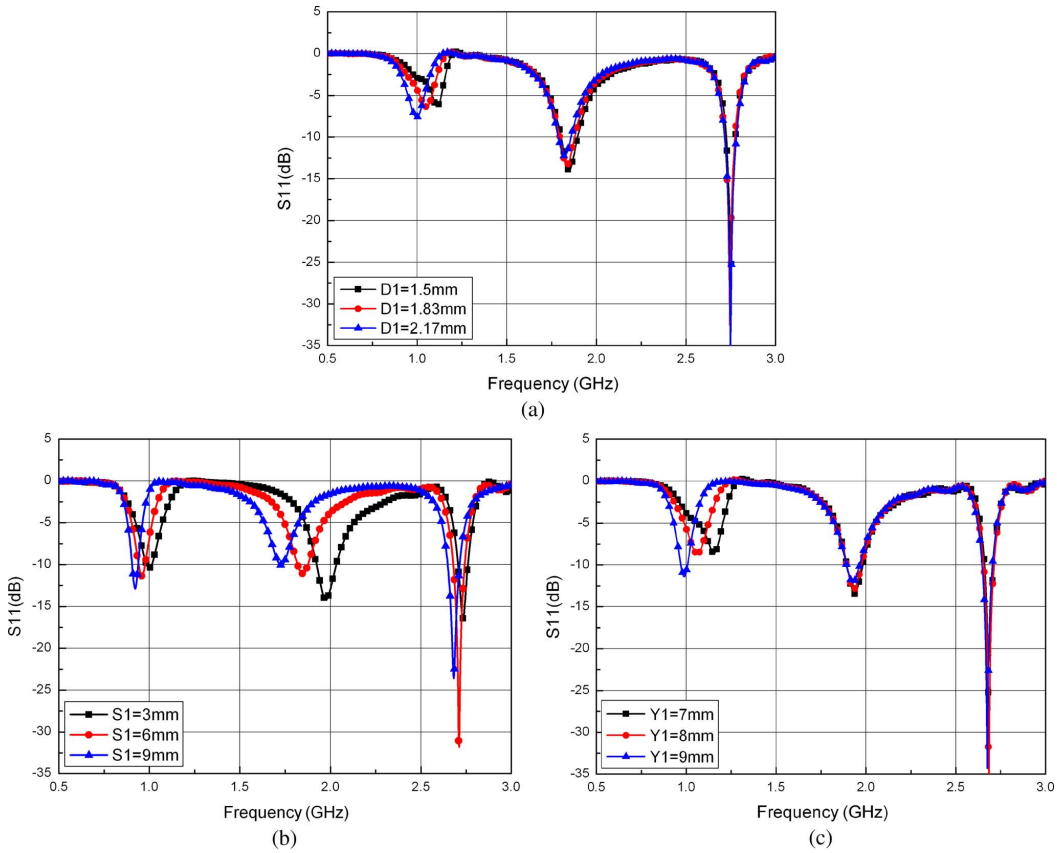

Fig. 4. Simulated results of return loss with variations of geometrical parameters (the folded part 1): (a) as a function of D1, (b) as a function of S1, and (c) as a function of Y1.

listed in literatures, it is well known that the resonance occurs at the quarter wavelength structure with current distributions. However, in the case of folded meander structure with slits inducing mutual cancellation of surface current flowing in reverse directions, it is necessary to design a little longer current path than a quarter-wavelength. From a basic principle with the folded part 1, the obtained parameter values for D1, H1, S1, and Y1 are listed in Table I with fixed width of slit, 0.6 mm. At the same time, the folded part 2 controlling Satellite DMB service is removed and replaced with flat radiator. Fig. 2(b) depicts that the only folded part 1 on top plate acts as a frequency controller of GSM900 band from a good agreement between two simulated results while the overall size of the top plate still maintains the resonant frequency of DCS1800 band.

C. The Effects of the Folded Part 2 Only

In a similar manner as shown in Section III-B, Satellite DMB (2605-2655 MHz) band can be resonated by employing the folded part 2 at the left bottom edged-line. The total area occupied by the folded part 2 is considerably smaller than that of the folded part 1 since the target frequency of the folded part 2 is higher than GSM900 frequency band. The geometrical parameters, D2, H2, S2, and Y2 constructing the folded part 2, are listed in Table I.

In a similar manner as shown in Section III-B, the dual-frequency antenna resonating at DCS1800 and Satellite DMB frequency bands can be designed by applying the meandered structure to the lower edge. From Fig. 2(c), it can be observed that the folded part 2 can generate another resonant frequency independently even though a little deviation between two analyses exists at the resonant frequency of Satellite DMB service band.

D. The Effects of Both the Folded Parts 1 and 2

According to the design procedure listed above, it is easily expected that three resonant frequencies covering GSM900, DCS1800, and Satellite DMB can be generated by applying both the folded parts 1 and 2 simultaneously and using independently operating characteristics of the proposed structure. Fig. 2(d) describes the return loss when both the folded parts 1 and 2 are employed simultaneously. It indicates that the overall size of top plate, the folded parts 1 and 2 generate the resonant frequencies at DCS1800, GSM900, and Satellite DMB, respectively.

Fig. 3(a) represents the current distribution flowing down the folded part 1 at the center frequency 0.92 GHz in GSM900 band. In order to generate the resonance at low frequency, it is necessary to achieve a long current path having a large area. This basic rule can explain the concentration of current distribution on the folded part 1. In a similar way, Fig. 3(b) depicts the current distribution on the folded part 2 generating the resonance at the center frequency 2.63 GHz of Satellite DMB band. At this time, the magnitude of current distributed on the folded part 1 is very weak. Hence, it is seen that the current distributions at different resonant frequencies are independently flowing down

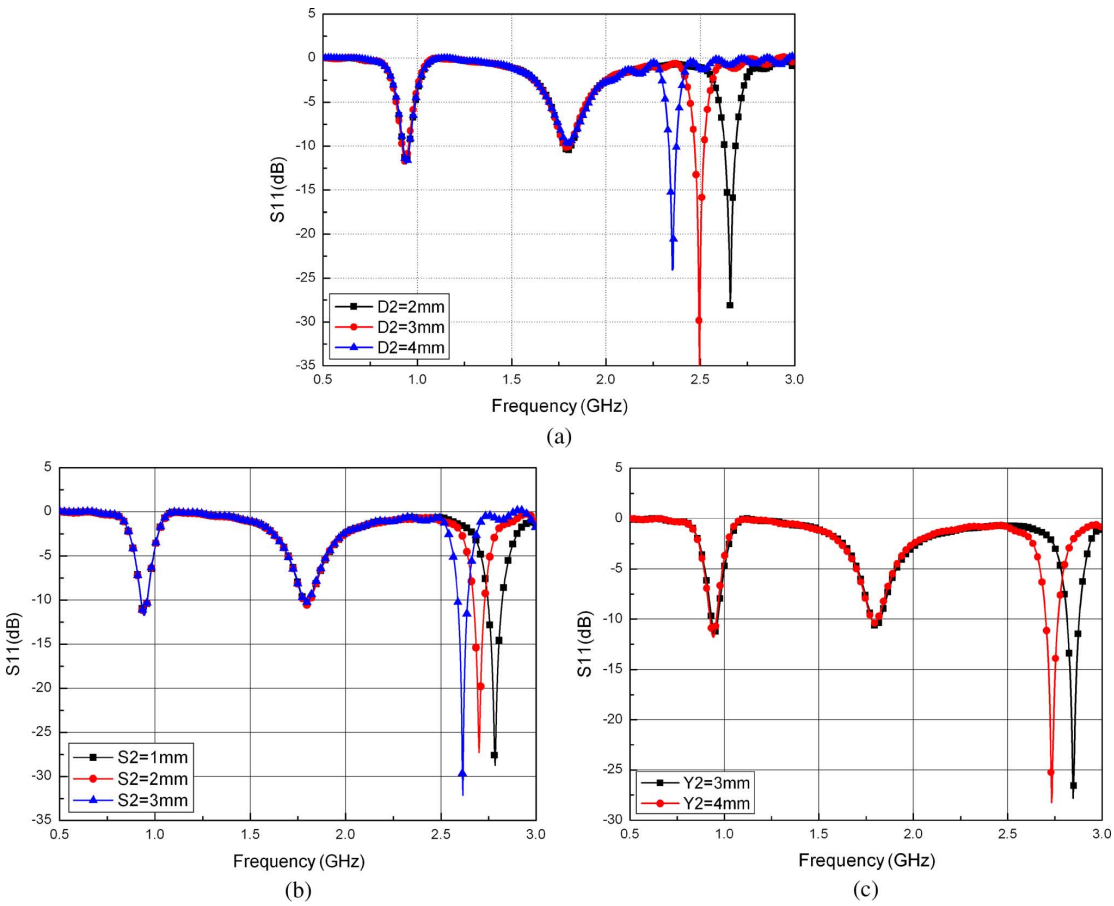

Fig. 5. Simulated results of return loss with variations of geometrical parameters (the folded part 2): (a) as a function of D2, (b) as a function of S2, and (c) as a function of Y2.

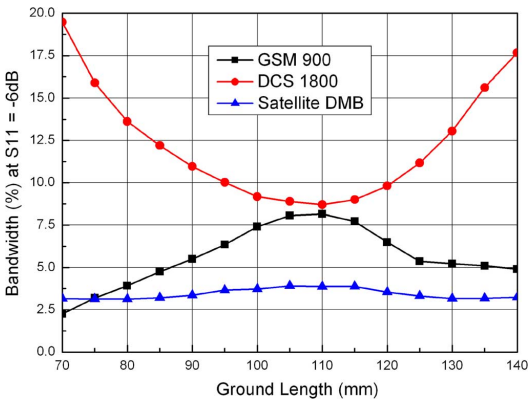

Fig. 6. Estimated bandwidth according to the length variation of ground plane.

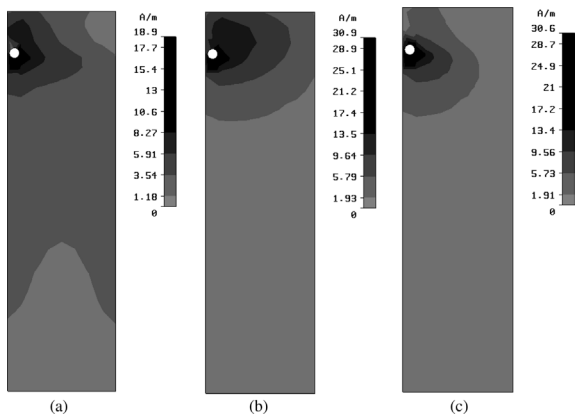

Fig. 7. Current distributions on the ground plane: (a) GSM900, (b) DCS1800, and (c) Satellite DMB.

the structure with a negligible coupling and are independently generated by perfectly different structures.

E. Variation of Design Parameters at the Folded Part 1

With the help of independently generating the resonant frequencies, the tri-band PIFA can be easily constructed. In order to check the frequency shift or bandwidth variation as a function of the design parameters, parametric studies at each control part have been carried out. Fig. 4(a)–(c) show the variation of the return losses according to the parameter changes.

Among them, Fig. 4(a) and (c) delineate that the resonant frequency moves to the lower as the width, D1, becomes wider and the length, Y1 gets longer. The reason is thought to be the increased current path due to the increased total area of the folded part 1. On the other hand, Fig. 4(b) indicates that the parameter, S1 affects both the resonant frequencies of GSM900, and DCS1800 simultaneously. These phenomena listed above depend on the variation of total slit size. D1 and Y1, leading to the variation of the total area of the folded part 1, does not change

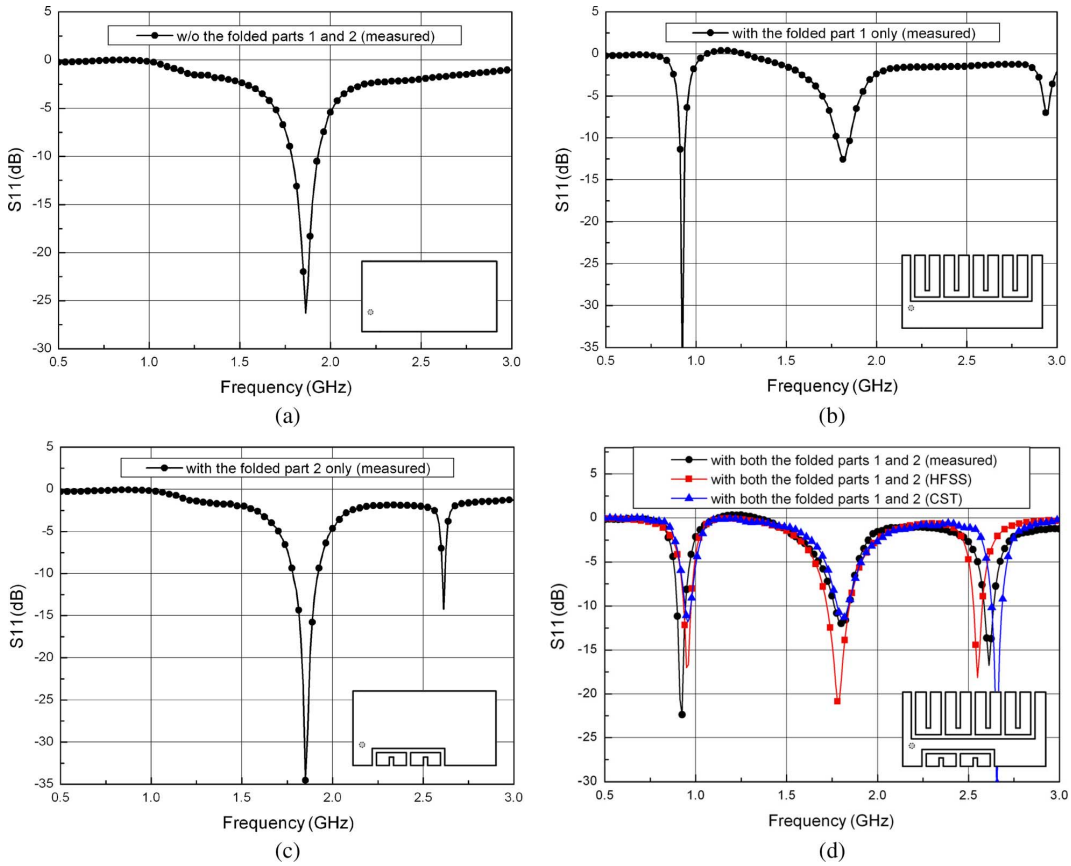

Fig. 8. Measured return loss according to the addition of radiating parts: (a) without the folded parts, (b) with the folded part 1 only, (c) with the folded part 2 only, and (d) with both the folded parts 1 and 2.

the total slit size while the variation of S1, changing the surface current path and including the frequency shift at GSM900 and DCS1800, does affect the total slit size. In addition to that, the various values of the design parameters, D1 and Y1 can control the resonant frequency and bandwidth in GSM900 band, but do not have an effect on the electrical performances in Satellite DMB band. This means that the resonance behavior of Satellite DMB is governed by not the higher-order mode of GSM900 band but the folded part 2.

As a result, an absolutely independent antenna not affecting DCS1800 and Satellite DMB but controlling GSM900 band can be easily constructed by choosing the length of S1 properly and using the other parameters, D1 and Y1.

F. Variation of Design Parameters at the Folded Part 2

In a similar way to Section III-E, the folded part 2 governing the resonant frequency of Satellite DMB band consists of the geometrical parameters, D2, S2, and Y2. Fig.5 (a)–(c) shows that controlling the parameters, D2, S2, and Y2 affects only the frequency shift of Satellite DMB band independently in having no relation with the movement of the other resonant frequencies. Additionally, Fig. 5(a) describes that the proposed antenna can be used for WLAN (2400-2483 MHz) band instead of Satellite DMB based on the return loss characteristics according to the appropriate variation of the given parameters.

G. The Effects of Ground Length

Usually the electrical characteristic of antenna such as impedance bandwidth is dependent on the feeding structure, the width and position of the shorting plate to a great extent. However, not only the geometrical parameter of antenna but also ground plane has an effect on the antenna performances. The ground effects caused by applying the variation of width and length of ground plane and inserting the slit and slot on the ground play an important role in a low frequency band especially. As a basic rule, the first maximum bandwidth can be obtained at the length corresponding to 1/3 of the resonant wavelength, λ. According to the basic rule, a simple calculation shows that the length of ground plane to satisfy the maximum bandwidth at GSM900 band can be represented as $110 + (160 \times \mathrm{n})$ mm $(\mathrm{n} = 0, 1, 2, \ldots)$ [9]. This formula can be also applied for the proposed antenna. Fig. 6 represents the effects of the length variation of ground plane on the impedance bandwidth using commercially available software. As expected, the bandwidth at GSM900 band is maximized when the length of ground plane is 110 mm. On the contrary, the bandwidth at DCS1800 band is minimized as a tradeoff relationship. However, in this paper the size of ground plane has been determined as 30×105 mm^2 focused on the wide impedance bandwidth at GSM band under the criterion of return loss less than -6 dB.

It can be also observed from Fig. 7 that the length of ground plane affects the impedance bandwidth in a view of current distributions on ground plane. The current density on ground plane

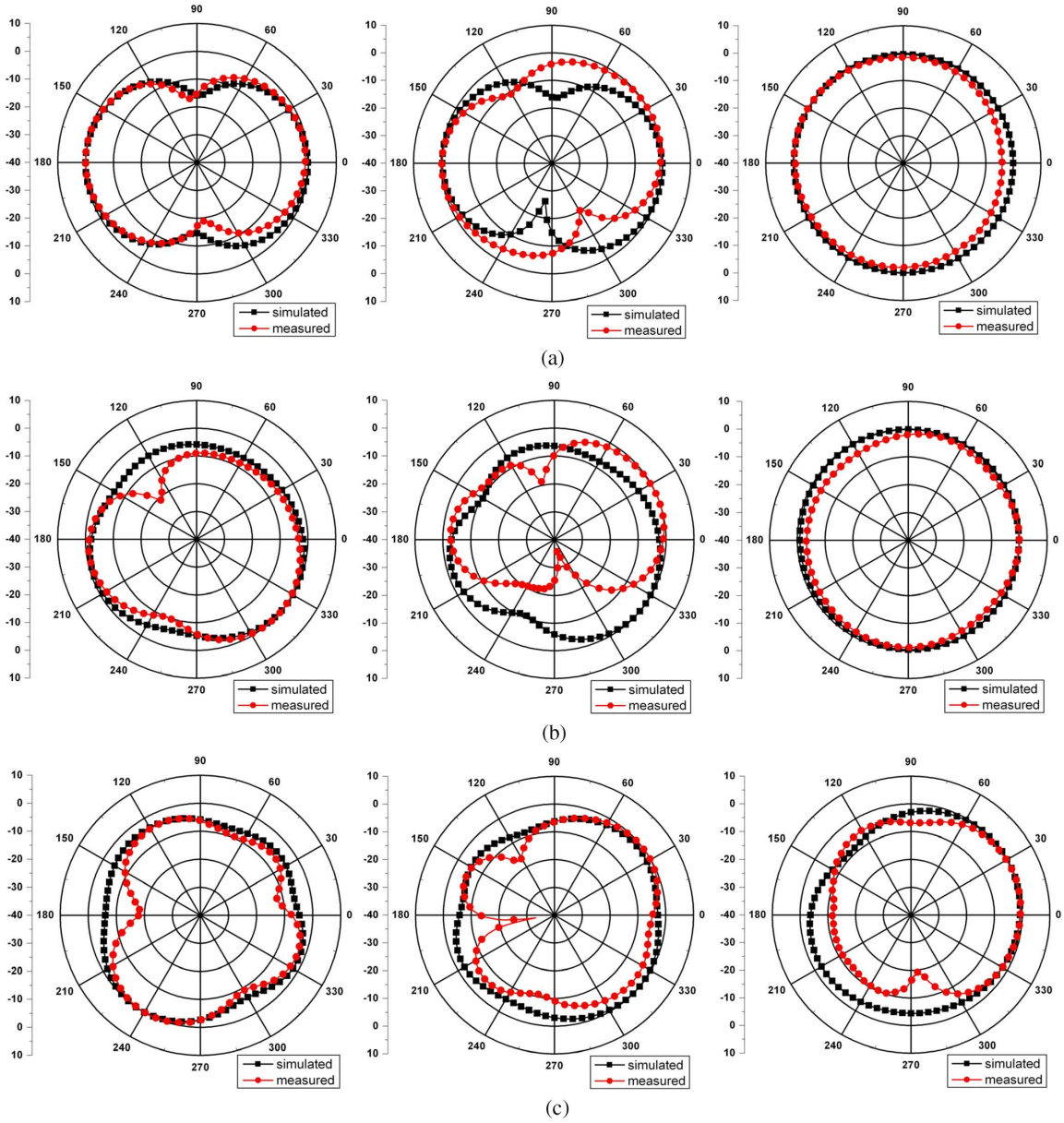

Fig. 9. Radiation patterns: (a) at $f = 0.92$ GHz ($x-y$, $y-z$, and $z-x$ plane), (b) at $f = 1.8$ GHz ($x-y$, $y-z$, and $z-x$ plane), and (c) at $f = 2.63$ GHz ($x-y$, $y-z$, and $z-x$ plane).

in Fig. 7(a) is more widely spread than those in Fig. 7(b) and (c) representing high current densities on near the feeding structure. In other words, it is necessary to ensure a little longer ground plane to obtain the satisfactory bandwidth in GSM900 band.

IV. Measurements and Verification

The expected return loss characteristics can be verified by measuring four cases consisting of only top plate, addition of the folded part 1 only, addition of the folded part 2 only, both addition of the folded parts 1 and 2. The employed material is a copper plate of thickness, 0.2 mm and the measurement has been carried out by using E5071B Network Analyzer of Agilent.

A. Measurement of PIFA With Only Top Plate

The estimated bandwidths obtained from two EM simulation tools are 282 MHz (1.715–1.997 GHz) and 370 MHz (1.63–2.0 GHz), respectively. From Fig. 8(a), it is clearly observed that the measured bandwidth is approximately 257 MHz covering from 1.73 to 1.987 GHz under the criterion of S_{11} less than -6 dB and the measured data is nearly the same as the predicted data.

B. Measurement of PIFA With Additional Folded Part 1

In this case, the parameters, D1, H1, S1, and Y1 constructing folded part 1 are set to be 2.5, 1, 7.3, and 9 mm, respectively, for optimized simulation and measurement. The expected first and second resonant frequencies are 0.942–1.026 GHz (BW = 84 MHz) and 1.756–1.936 GHz (BW = 180 MHz) for CST MW Studio and 0.93–1.01 GHz (BW = 80 MHz) and 1.7–1.95 GHz (BW = 250 MHz) for HFSS, respectively. The measured data shown in Fig. 8(b) indicate that the first and second resonant frequencies are 0.897–0.957 GHz (BW = 60 MHz)

TAble II
SIMULATED AND MEASURED MAXIMUM GAINS

Frequency (GHz)	GSM900	DCS1800	Satellite DMB
Simulated Max. Gain (dBi)	f = 0.955	f = 1.807	f = 2.65
	2.0	3.4	3.1
Measured Max. Gain (dBi)	f = 0.92	f = 1.8	f = 2.63
	1.19	2.93	1.48

and 1.726–1.907 GHz (BW = 181 MHz), respectively, representing a good agreement with the expected data.

C. Measurement of PIFA With Additional Folded Part 2

The antenna configuration of this case is constructed by applying the folded part 2 only to the top plate without the folded part 1. As estimated from Fig. 2(c), the simulated data for the first and second resonant frequencies are 1.699–1.949 GHz (BW = 250 MHz) and 2.582–2.657 GHz (BW = 75 MHz) using CST MW Studio and 1.61–1.98 GHz (BW = 370 MHz) and 2.52–2.56 GHz (BW = 40 MHz) using HFSS, respectively. For the fabrication and measurement, the optimized parameters, D2, H2, S2, and Y2 building-up the folded part 2 are determined as 3, 1, 2, and 3.8 mm, respectively. The measured datum in Fig. 8(c) shows that the first and second resonant frequencies are 1.726–1.967 GHz (BW = 241 MHz) and 2.686–2.716 GHz (BW = 30 MHz), respectively. It is seen that this configuration can generate dual-resonant frequencies with a little narrower bandwidth rather than the expected values.

D. Measurement of PIFA With Both the Folded Parts 1 and 2

As a final goal, the measurement of PIFA generating tri-band resonant frequencies has been carried out under the criterion of return loss less than −6 dB. Fig. 8(d) shows the reflection characteristics of tri-band PIFA covering the frequency bands, GSM900 (878–957 MHz, BW = 79 MHz), DCS1800 (1700–1882 MHz, BW = 182 MHz) and Satellite DMB (2560–2660 MHz, BW = 100 MHz). From the above results, it is guaranteed that tri-band antenna working at each resonant frequency with independent frequency-control structures can be easily constructed according to the described design procedures.

The measured and simulated radiation patterns at the center frequencies 0.92, 1.8, and 2.63 GHz of three service bands are plotted and compared according to the cutting plane in Fig. 9(a)–(c). The radiation patterns in $z-x$ plane are nearly omnidirectional characteristics. Thus, it means that the proposed antenna can be used in hand-held mobile systems. The measured maximum gains are 1.19, 2.93, and 1.48 dBi at 0.92, 1.8, and 2.63 GHz, respectively, with the estimated gains, 2.0, 3.4, and 3.1 dBi at 0.995, 1.807, 2.65 GHz using EM simulation tool as shown in Table II.

As another key performance in antenna design, consider the total radiation efficiency concerned with input mismatching and radiation loss. Fig. 10(a) plots the return loss characteristic and total efficiency at the same time. It is seen that the total efficiencies are very high at the three resonant frequencies and

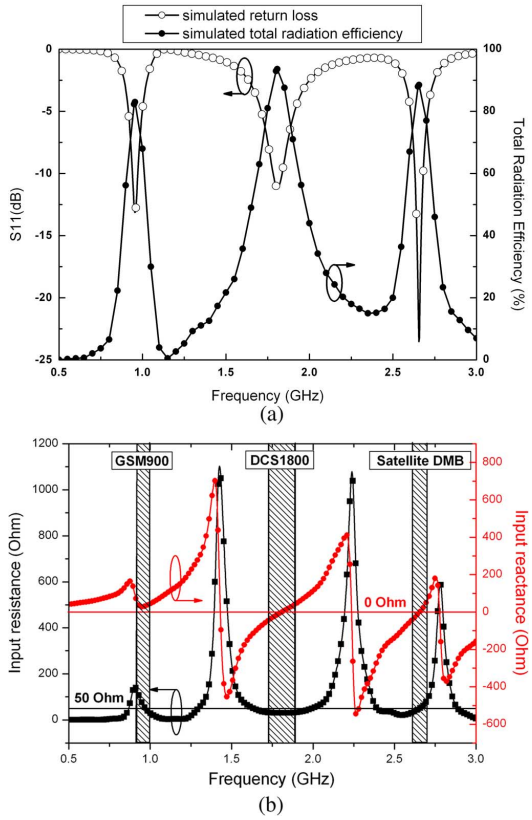

Fig. 10. Simulated (a) total radiation efficiency as a function of frequency when the optimized parameters for a tri-band PIFA are applied and (b) input impedance.

amount to more than 80% (GSM900 and Satellite DMB) and 90% (DCS1800), respectively. From Fig. 10(b) showing the input impedance of the proposed antenna at three different service bands, it is confirmed that the input resistance and reactance are approaching to 50-Ω and 0-Ω, respectively, at each resonant frequency.

V. CONCLUSION

A novel and useful design procedure for tri-band PIFA covering GSM900, DCS1800, and Satellite DMB has been illustrated. The resonant characteristics of the proposed antenna having a total volume of $30 \times 16 \times 9$ mm^3 have been predicted and verified by using not only Full EM simulation tools, CST MW Studio and HFSS but also measurement of four independent antenna structures. Under the criterion of VSWR less than 3, it is found that the proposed antenna covers three service bands with percentage bandwidth, 8.6% (878–957 MHz), 10.2% (1700–1882 MHz) and 3.8% (2560–2660 MHz). In addition to that, it has been verified that the folded parts 1 and 2 on the top plate can independently control the resonant frequencies at GSM900 and Satellite DMB bands, respectively, while the DCS1800 band is under the control of the total size of the top plate.

The measured data show that good radiation patterns in three cutting planes are obtained with maximum gains, 1.19, 2.93, and 1.48 dBi at 0.92, 1.8, and 2.63 GHz, respectively, with the predicted total radiation efficiency more than 80%. Thus, the

proposed antenna and design procedure can be used for handheld wireless systems.

REFERENCES

[1] Z. M. Chen and Y. W. M. Chia, Eds., *Broadband Planar Antennas Design and Applications*. New York: Wiley, 2006, ch. 4.

[2] W. P. Dou and Y. W. M. Chia, "Novel meandered planar inverted-F antenna for triple-frequency operation," *Microw. Opt. Technol. Lett.*, vol. 27, no. 1, pp. 58–60, Oct. 2000.

[3] P. Salonen, M. Keskilammi, and M. Kivikoski, "Single-feed dual-band planar inverted-F antenna with U-shaped slot," *IEEE Trans. Antennas Propag.*, vol. 48, no. 8, pp. 1262–1264, Aug. 2000.

[4] H. Park, K. Chung, and J. Choi, "Design of a planar inverted-F antenna with very wide impedance bandwidth," *IEEE Microw. Wireless Compon. Lett.*, vol. 16, no. 3, pp. 113–115, Mar. 2006.

[5] P. Ciais, R. Staraj, G. Kossiavas, and C. Luxey, "Design of an internal quad-band antenna for mobile phones," *IEEE Microw. Wireless Compon. Lett.*, vol. 14, no. 4, pp. 148–150, Apr. 2004.

[6] M. K. Kärkkäinen, "Meandered multiband PIFA with coplaar parasitic patches," *IEEE Microw. Wireless Compon. Lett.*, vol. 15, no. 10, pp. 630–632, Oct. 2005.

[7] M. F. Abedin and M. Ali, "Modifying the ground plane and its effect on Planar Inverted-F Antennas (PIFAs) for mobile phone handsets," *IEEE Antennas Wireless Propag. Lett.*, vol. 2, pp. 226–229, 2003.

[8] K. L. Virga and Y. Rahmat-Samii, "Low-profile enhanced-bandwidth PIFA antennas for wireless communications packaging," *IEEE Trans. Microw. Theory Tech.*, vol. 45, no. 10, pp. 1879–1888, Oct. 1997.

[9] B. J. Herting, A. Perrotta, and J. T. Bernhard, "Finite ground plane packaging effects on a dual-band PIFA," in *Proc. IEEE Topical Meetings on Electrical Performance of Electronic Packaging*, Oct. 2002, pp. 95–98.

[10] Z. D. Liu, P. S. Hall, and D. Wake, "Dual-frequency planar inverted-F antenna," *IEEE Trans. Antennas Propag.*, vol. 45, no. 10, pp. 1451–1458, Oct. 1997.

[11] D. Kim, J. W. Lee, C. S. Cho, and J. Kim, "A compact tri-band PIFA with multiple-folded parasitic elements," in *Proc. IEEE MTT-S Int. Microwave Symp.*, 2007, pp. 259–262.

[12] CST Microwave Studio (MWS) ver. 5, CST Corporation.

[13] High Frequency Structure Simulator (HFSS) ver. 10, Ansoft Corporation.

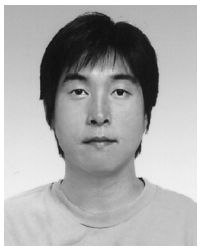

Dong-yeon Kim received the B.S. degree in electronics, telecommunications, and computer engineering, from Korea Aerospace University, Goyang, Korea, in 2007, where he is currently working toward the M.S. degree.

His research interests include multiband antenna design and electromagnetic interference (EMI)/electromagnetic compatibility (EMC) on printed circuit boards (PCBs).

Jae W. Lee (S'92–M'98) received the B.S. degree in electronic engineering from Hanyang University, Seoul, Korea, and the M.S. and Ph.D. degrees in electrical engineering (with an emphasis in electromagnetics) from Korea Advanced Institute of Science and Technology (KAIST), Taejon, Korea, in 1992, 1994, and 1998, respectively.

From 1998 to 2004, he was a senior member in the Advanced Radio Technology Department, Radio and Broadcasting Research Laboratory, Electronics and Telecommunications Research Institute (ETRI), Taejon. He later joined the School of Electronics, Telecommunications and Computer Engineering, Korea Aerospace University, Korea, where he is currently an Assistant Professor. His research interests include high power amplifier design, computational electromagnetics, EMI/EMC analysis on PCB, and component design in microwave and millimeter-wave.

Choon Sik Cho (S'98–M'99) received the B.S. degree in control and instrumentation engineering from Seoul National University, Seoul, Korea, in 1987, the M.S. degree in electrical and computer engineering from the University of South Carolina, Columbia, in 1995, and the Ph.D. degree in electrical and computer engineering from University of Colorado at Boulder, in 1998.

From 1987 to 1992, he was with LG Electronics, where he was involved with communication systems. From 1999 to 2003, he was with Pantec & Curitel, where he was principally involved with the development of mobile phones. In 2004, he joined the School of Electronics, Telecommunication and Computer Engineering, Korea Aerospace University, Goyang, Korea. His research interests include the design of RF integrated circuit (RFICs)/monolithic microwave integrated circuit (MMICs), especially for power amplifiers, oscillators, low-noise amplifiers (LNAs), antennas and passive circuit design, and the computational analysis of electromagnetics.

Taek K. Lee (S'83–M'90) was born in Gyeongbuk, Korea, on January 11, 1958. He received the B.S. degree in electronic engineering from Korea University, Seoul, Korea, in 1983, and the M.S. and Ph.D. degrees in electrical engineering from the Korea Advanced Institute of Science and Technology, Seoul, in 1985 and 1990, respectively.

From May 1990 to April 1991, he was a Postdoctoral Fellow with the University of Texas at Austin (under a grant from the Korea Science and Engineering Foundation). From August 1991 to February 1992, he was with the Korea Advanced Institute of Science and Technology. In March 1992, he joined the faculty of Korea Aerospace University, Goyang, Korea, where he is currently a Professor with the School of Electronics, Telecommunication, and Computer Engineering. From July 2001 to July 2002, he was an Associate Visiting Research Professor with the University of Illinois at Urbana-Champaign. His research interests include computational electromagnetics, antennas, analysis and design of microwave passive circuits, and geophysical scattering.